

Diel Variability Affects the Inorganic Marine Carbon System in the Sea-Surface Microlayer of a Mediterranean coastal area (Šibenik, Croatia)

Ander López-Puertas^{1, 2}, Oliver Wurl¹, Sanja Frka³, Mariana Ribas-Ribas¹

¹ Center for Marine Sensors (ZfMarS), Institute for Chemistry and Biology of the Marine Environment (ICBM), School of Mathematics and Science, Carl von Ossietzky Universität Oldenburg, Ammerländer Heerstraße 114-118, 26129 Oldenburg, Germany

² Instituto Universitario de Investigación Marina (INMAR), Universidad de Cádiz, 11510, Puerto Real, Cádiz, Spain

³ Laboratory for Marine and Atmospheric Biogeochemistry, Division for Marine and Environmental Research, Ruder Bošković Institute, Bijenicka c. 54, 10000 Zagreb, Croatia

Correspondence to: Ander López-Puertas (ander.lopezpuertas@uca.es)

Código de campo cambiado

Abstract

The ocean plays a crucial role in the global carbon cycle by absorbing and storing ~~substantial amounts~~about one-third of ~~anthropogenic~~atmospheric carbon dioxide (CO₂). It is estimated that the ocean has sequestered approximately 26% of CO₂ emissions over the last decade, resulting in significant changes in the marine carbon system and impacting the marine environment. The sea-surface microlayer (SML) plays a crucial role in these processes, facilitating the transfer of ~~materials~~matter and energy between the ocean and the atmosphere. However, most studies on the carbon cycle in the SML have primarily addressed daily variability and overlooked nocturnal processes, which may lead to inaccurate global carbon estimates. We analysed temperature, salinity, pH_{T25}, and pCO₂ using data collected over three complete diel cycles during an oceanographic campaign along the Croatian coast near Šibenik in the Middle Adriatic. Our analysis revealed statistically significant differences (p < 0.05) between daytime and nighttime measurements of temperature, salinity, and pH_{T25}. These differences may be related to the occurrence of buoyancy fluxes, which are typically more pronounced during the day and could enhance CO₂ fluxes, as observed with values of $1.98 \pm 2.52 \text{ mmol cm}^{-2} \text{ h}^{-1}$ during the day, while at night, they dropped to $0.01 \pm 0.02 \text{ mmol cm}^{-2} \text{ h}^{-1}$. These findings emphasise the importance of considering complete diurnal cycles to accurately capture the variability in thermohaline features and carbon exchange processes, thereby improving our understanding of the ~~role of the ocean~~ocean's role in climate change.

1. Introduction

The ocean is a crucial climate regulator that mitigates the effects of anthropogenic emissions (Gattuso *et al.*, 2015). It absorbs ~~a significant portion~~more than 90% of the Earth's excess heat (Hoegh-Guldberg *et al.*, 2014).

Con formato: Fuente: 10 pto

Con formato: Fuente: 10 pto

Con formato: Fuente: 10 pto

Con formato: Fuente: 10 pto

Con formato: Fuente: 10 pto

Con formato: Fuente: 10 pto

Con formato: Fuente: 10 pto

Con formato: Fuente: 10 pto

Con formato: Inglés (Estados Unidos)

35 ~~Pörtner et al., 2019~~) and captures ~~about~~approximately one-third of a substantial amount of anthropogenic carbon
dioxide (CO₂) emissions (~~Pörtner et al., 2019; Wong et al., 2014~~). It is well known that CO₂ ~~significantly~~
~~affects marine seawater chemistry~~ (Doney et al., 2009; Gattuso et al., 2015), and it is estimated that the ocean
has sequestered approximately 26% of global CO₂ emissions in ~~has~~ a significant impact on seawater chemistry
40 (Doney et al., 2009; Gattuso et al., 2015). It is estimated that the ocean has sequestered approximately 26% of
global CO₂ emissions over the last decade (Friedlingstein et al., 2024). Consequently, changes in the ocean
environment have exceeded the magnitude and rate of natural variation due to anthropogenic carbon perturbation
over the last millennia (Gattuso et al., 2015). In this context, the marine carbon system undergoes substantial
modifications, resulting in various effects on the marine environment, including a decrease in pH levels (~~Cantoni~~
~~et al., 2012; Doney et al., 2009; IPCC, 2023; Orr et al., 2005~~). Therefore, understanding the evolving state of
marine biogeochemistry in the context of climate change is crucial, with a primary focus on the upper layers of
45 the water column, which are closely linked to ocean-atmosphere interactions.

Con formato: Inglés (Estados Unidos)

Con formato: Subíndice

In the ocean-atmosphere system, the sea-surface microlayer (SML) plays a vital role in transferring materials and
energy, such as heat, gases, and particles (Wurl et al., 2019), which must pass through it (Frka et al., 2009; Stolle
et al., 2020). The SML is a distinctive and complex marine environment that represents the interfacial boundary
layer between the ocean and the atmosphere (Cunliffe et al., 2013; Frka et al., 2009; Wurl et al., 2011). Its
50 thickness typically does not exceed 1000 µm, and it exhibits distinct biological and physicochemical properties
compared with the underlying water masses (Cunliffe et al., 2013; Stolle et al., 2020; Wurl et al., 2011). Thus,
the SML experiences instantaneous meteorological forcing, such as solar radiation, wind, and atmospheric inputs
(Wurl et al., 2019; Gassen et al., 2023), which impacts the development of physical and biogeochemical
processes occurring in the underlying water (Liss & Duce, 1997; Stolle et al., 2020, Engel et al 2017; Mustaffa
55 et al., 2020; Wurl et al., 2017). These characteristics of the SML overlap with the growing interest in
oceanographic research to study the spatiotemporal variability of the marine carbon system (Cantoni et al.,
2016), as this layer is essential for understanding global marine biogeochemistry. However, to gain a
comprehensive spatiotemporal perspective on marine carbon chemistry processes, focusing on underexplored
fields, such as the role of nocturnal processes within the diel cycle, is crucial.

Con formato: Español (España)

Con formato: Sin Resaltar

60 Daily variations force cyclic changes in chemistry (De Montety et al., 2011), which are influenced by processes
such as photosynthesis, ~~air-sea gas exchange between the ocean and atmosphere~~, and various environmental
conditions (e.g., light, temperature, and nutrient availability) (Poulson & Sullivan, 2010). These processes
directly affect the seawater pH by adding or removing CO₂ from seawater (Poulson & Sullivan, 2010; Takahashi
et al., 2002). It is well known that photosynthesis consumes CO₂ during the day, thereby reducing pCO₂ levels,
65 and consequently causing an increase in pH (Cantoni et al., 2012; Takahashi et al., 2002). At night, the CO₂
produced by respiration tends to be more constant and accumulates in the water column, leading to an increase in
pCO₂ and a decrease in pH (Cantoni et al., 2012, del Giorgio & Williams, 2005; Shaw et al., 2013; Gattuso et al.,
1999). Although these processes are significant for seawater chemistry, research has predominantly focused on
diurnal processes. As a result, the roles of respiration and other nocturnal processes in the SML remain largely
70 unexplored (Yates et al., 2007).

Within this framework, the Mediterranean Sea presents a unique research opportunity to investigate the
spatiotemporal variability of the marine carbon system. It is often referred to as a "laboratory basin"

(Bergamasco & Malanotte-Rizzoli, 2010; Robinson & Golnaraghi, 1994) because it ~~allows us to approximate processes occurring on a global scale within a shorter time and enables us to approximate processes occurring on a global scale within a shorter timeframe and smaller space~~ (Álvarez *et al.*, 2014). Despite representing 0.8% of the global ocean surface (Álvarez-Rodríguez, 2012), the Mediterranean Sea is considered an important anthropogenic carbon storage (Álvarez *et al.*, 2014), as it absorbs a disproportionally larger amount of anthropogenic carbon compared to the global ocean (Hassoun *et al.*, 2015; Schneider *et al.*, 2010). Higher acidification ranges (-0.001 to -0.009 pH unit yr⁻¹) (Hassoun *et al.*, 2022) were measured and exceeded those measured in the Atlantic Ocean (-0.001 to -0.0026 pH unit yr⁻¹) (Takahashi *et al.*, 2014), ~~in line with regional coastal studies showing strong acidification trends in the Mediterranean (Kapsenberg *et al.* 2017)~~. However, as explored in this study, the dynamics of biogeochemical processes in coastal regions are more complex than those in the open ocean (Borges, 2005). When examining oceanic regions, it is ~~essential to recognise that daily variability has a profound impact on~~ marine carbon chemistry.

This study emphasises the role of diel variability in thermohaline features and dynamics of the marine inorganic carbon cycle in the coastal region of the Mediterranean Sea (Šibenik, Croatia), thereby providing a comprehensive understanding of the processes that influence the complete diurnal cycle. Therefore, it is essential to incorporate nocturnal processes into global estimates of marine carbon cycle dynamics. We present high-resolution data to understand biogeochemical processes and their variability in the water column, which complicates predictions of ~~coastal marine carbon system variations~~ ~~variations in the coastal marine carbon system~~ (Cantoni *et al.*, 2012). We have focused on understanding the nocturnal processes that affect the inorganic carbon system, thereby helping to clarify the uncertainties associated with this system. This study contributes to the identification of anthropogenic influences on the marine environment in the context of climate change.

2. Materials and Methods

2.1. Sampling Strategy and Seawater Analyses

Sampling was conducted ~~in the lower estuary of the Krka River (central-eastern Adriatic), immediately offshore from the St. Anthony Channel, in the Middle Adriatic region, specifically on the Croatian coast near Šibenik (Figure 1). The estuary is highly stratified and exhibits microtidality, extending about 23 km inland, with depths increasing from less than 2 m at the head to about 42 m at the mouth (Cukrov, 2024; Prohic approximately 23 km inland, with depths increasing from less than 2 m at the head to around 42 m at the mouth (Cukrov, 2024; Prohic, 1989). Similar to other Mediterranean estuaries, tidal ranges are small (0.2-0.5 m) and result, resulting in minimal currents and stable vertical stratification, with freshwater or brackish water flowing over a lower marine layer (Cukrov, 2024). Average annual river discharge is ~50 m³ s⁻¹, varying seasonally from ~ 5 to 480 m³ s⁻¹ (Cukrov, 2024; Bužančić *et al.*, 2016; Marcinek *et al.*, 2020). Previous studies in the area have reported that water residence times range from a few days in winter to several weeks in summer, depending on the hydrodynamics of the freshwater or marine layers (Žutić and Legović, 1987; Cetninc *et al.*, 2004). During the sampling period (August 10–15, 2020), precipitation was very low, averaging 1.4 mm over the first half of August (Croatian Meteorological and Hydrological Service (2020), consistent with the dry summer conditions~~

110 typical for the region. This environment provided ideal stable conditions for assessing the daily variability of
SML and ULW parameters with minimal interference from tides or precipitation.

Temperature, conductivity, and pH data from the SML were collected using sensors integrated in a flow-through
system on the “Sea Surface Scanner (S³)” (Ribas-Ribas *et al.*, 2017). The S³ is a 4.5 m long and 2.2 m wide
uncrewed catamaran, remotely piloted by radio control from a small support vessel, ~~with no personnel on board~~
115 during a six-day campaign in August 2020 (from 10 to 15 August 2020). As specified in Ribas-Ribas *et al.*
(2017), the system features rotating glass discs ~~that at which adhere to the SML water adheres to on which the~~
SML water adheres via surface tension. ~~where a~~ A set of scraping mechanisms on the immersed side collects the
adhering water and transfers it to a closed, ~~continuous flow system, minimizing continuous-flow system,~~
minimising atmospheric contact. Measurements of the underlying water (ULW; ~1 m) were performed similarly.
120 Underlying water (ULW) was continuously collected at a depth of 1 m through a rigid inlet pipe. Both SML and
ULW water were pumped directly to the onboard sensor and sampler system. In addition, the S³ carried an
automated water collector (Table 1) with twenty-four 1-L polypropylene bottles, which could be filled remotely
with SML or ULW water, allowing discrete samples to be collected during transects. Discrete samples for
inorganic carbon parameters (DIC and TA) were collected separately in bottles (250 mL), ~~taken directly from the~~
125 S³ outlets by approaching directly from the S³ outlets, ~~approached by the catamaran with the support zodiac, and~~
immediately sealed to prevent atmospheric contamination.

Field deployments of the S³ were conducted six times per diel cycle between 10 and 15 August 2020, with each
deployment lasting 30–45 minutes. Although the catamaran moved along short transects within the sampling
area, for analytical purposes, the sampling location was treated as a single point, since spatial variations within
130 the ~~area~~ region were minimal. Sensors recorded temperature, conductivity, and pH from both SML and ULW at
30-second intervals. Specifically, the pH was measured using the integrated sensor of the S³ flow-through system
(Ribas-Ribas *et al.*, 2017) and is reported on the total scale. The uncertainties of the measured temperature,
conductivity and pH were estimated based on sensor specifications (Table 1). Solar radiance and wind data were
collected from a meteorological station (Davis Instruments, Vantage Pro2 Plus) located on Zlarin Island. This
135 study collected high-volume samples of approximately 15 L from the SML and ULW for comprehensive
analyses related to the SML. Discrete samples designated for the inorganic carbon parameters were collected
directly from the S³ output and immediately sealed to prevent atmospheric contamination. For the analysis, a
total of These measurements were conducted six times per diel cycle, each lasting 30–45 minutes, with a
sampling frequency of 30 seconds. Three diurnal cycles were sampled, ~~conducted during the study period. In~~
140 each cycle, four deployments were conducted during daytime conditions (diurnal data), and two deployments
were performed at night (nocturnal data). Environmental conditions during the campaign were typical for the
region, with no significant rainfall events. This deployment strategy ~~allowed representative sampling of the study~~
~~area while minimizing~~ enabled representative sampling of the study area while minimising the potential influence
of microtidal variations on the SML and ULW measurements. ~~the first four measurements were taken during~~
145 periods of noticeable solar radiation (diurnal data), whereas the last two occurred without solar radiation
(nocturnal data).

Con formato: Fuente: Sin Negrita, Sin Cursiva

Código de campo cambiado

Con formato: Sin Resaltar

Con formato: Sin Resaltar

Con formato: Superíndice

Con formato: Superíndice

Con formato: Fuente: Sin Negrita

150 Subsamples from the SML and ULW were collected in high-density polyethylene (HDPE) bottles to determine the phosphate (PO_4^{3-}) and silicate $[\text{Si}(\text{OH})_4]$ concentrations. To preserve the samples, mercury chloride (HgCl_2) was added. The preserved samples were stored at $+4^\circ\text{C}$ until further analysis in the laboratory. Nutrient concentrations were measured using a sequential automatic analyser (SAA, SYSTEAS EASYCHEM) according to the standard protocols described by Laskov *et al.*, (2007) and Fanning & Pilson, (1973). These nutrient data were subsequently used as inputs for calculating partial pressure of CO_2 ($p\text{CO}_2$) with the CO_2Sys program (Version v3.2.0, MATLAB) (Sharp *et al.*, 2020; Van Heuven *et al.*, 2011).

155 Table 1. Manufacturers, models, and specifications of the sensors employed to measure pH, salinity, and temperature in the sea-surface microlayer (SML) and underlying water (ULW). Adapted from Ribas-Ribas *et al.*, (2017).

Parameter	Manufacturer	Model	Range, unit, and resolution	Accuracy	Sample
pH	VWR	MU 6100 H	-2.000 to 19.999	± 0.005	SML and ULW
Salinity	VWR	MU 6100 H	0.0-70.0	$\pm 0.2\%$	SML and ULW
Temperature	VWR	MU 6100 H	-5.0° to 105.0°C	$\pm 0.1^\circ\text{C}$	SML and ULW

Con formato: Fuente: Cursiva

Con formato: Fuente: Negrita, Sin Cursiva

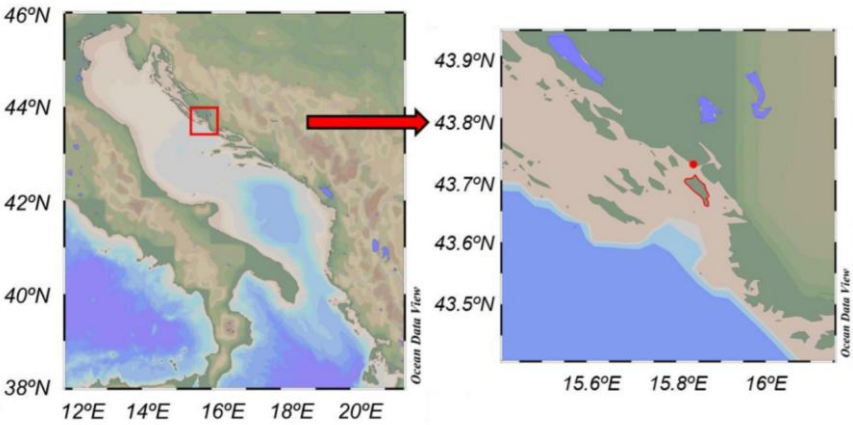
Con formato: Fuente: Sin Cursiva, Inglés (Estados Unidos)

Con formato: Descripción, Conservar con el siguiente

Con formato: Fuente: Sin Cursiva

Con formato: Fuente: Negrita, Sin Cursiva

Tabla con formato



160 Figure 1. Map of the sampling area in the Middle Adriatic Sea, created using Ocean Data View (Schlitzer, 2022). The red dot indicates the sampling area, whereas Zlarin Island, where the meteorological station is situated, is outlined in red.

2.2. Marine Carbon System Determination

165 DIC samples (20 mL) were analysed by coulometric titration (CM 5014, UIC, USA) with an excess of 10% phosphoric acid. Total Alkalinity (TA) samples (100 mL) were measured via potentiometric titration (916 Ti-

Touch, Metrohm, Switzerland) and calculated using a modified Gran plot approach implemented in Calculate (version 1.8.0) (Humphreys *et al.*, 2022). Calibration was performed with certified reference material (Batch 187) obtained from A. G. Dickson at the Scripps Institution of Oceanography. The 1 σ measurement precision was $\pm 3 \mu\text{mol kg}^{-1}$ for DIC and $\pm 2 \mu\text{mol kg}^{-1}$ for TA.

To eliminate the effects of temperature variation on the results, the pH values measured in the seawater samples were adjusted to the average temperature value of 25.43 °C, hereafter referred to as pH_{T25}. The normalisation utilised an adjustment factor of 0.018 pH units per °C, which is widely accepted for the range of pH and TA conditions typical of seawater (Eq. 1) (Dickson *et al.*, 2007; Dickson & Millero, 1987; Zeebe & Wolf-Gladrow, 2001):

$$pH_{T25} = pH + (T - 25.43) \cdot 0.018 \quad (1)$$

To evaluate the marine carbon system, ~~the partial pressure of CO₂ ($p\text{CO}_2$)~~ was calculated with the CO2SYS program (Version v3.2.0, MATLAB) (Sharp *et al.*, 2020; Van Heuven *et al.*, 2011) using as input parameters: DIC; TA, PO₄³⁻, and Si(OH)₄; salinity (S); temperature (T), and pressure. The respective dissociation constants were used for carbon (Mehrbach *et al.*, 1973), sulfate (KSO₄) (Dickson & Millero, 1987), fluorine (KF) (Perez & Fraga, 1987), and the borate-salinity ratio (Lee *et al.*, 2010). Missing $p\text{CO}_2$ values were due to erroneous DIC and/or TA measurements. Consequently, standard deviations could not be calculated when the number of reliable data points was less than three. Once the $p\text{CO}_2$ values were calculated, the CO₂ flux through the ocean-atmosphere interface in the monitoring area was estimated using the following equation:

$$F = \Delta p\text{CO}_2 \cdot k \cdot \alpha \quad (2)$$

where F is the CO₂ flux (mmol m⁻² d⁻¹), $\Delta p\text{CO}_2$ is equal to the difference in the partial pressures of the gas between the surface water and the atmosphere, k is the gas transfer coefficient (cm h⁻¹) from Wanninkhof (2014), and α is the solubility of CO₂ in seawater (mol L⁻¹ atm⁻¹). To calculate the partial pressure gradient of CO₂, atmospheric $p\text{CO}_2$ data were ~~obtained as the monthly mean for August 2020 sourced from the ICOS Lampedusa atmospheric station~~ Mauna Loa Observatory, which provides quality-controlled dry-air CO₂ measurements representative of the Mediterranean region (di Sarra *et al.*, 2025). ~~To quantify the bias introduced when nocturnal fluxes were ignored, we compared daily means including all valid data from each cycle with means based only on daytime measurements. The percentage error was defined as $\left(\frac{F_{\text{daytime}} - F_{\text{diel}}}{F_{\text{diel}}}\right) \times 100$, with both means calculated as arithmetic averages of available fluxes. This approach explicitly evaluates the uncertainty in daily estimates when nocturnal processes are excluded (Garbe *et al.*, 2014). The percentage error associated with excluding nocturnal fluxes in the daily average calculation was determined by comparing the mean fluxes calculated with and without nocturnal data, expressed as the relative difference between the two values.~~

2.3. Salinity and density correction

To ensure high-quality data, a correction factor (CF) was applied to the continuous salinity and pH_{T25} data. Discrete salinity values obtained from laboratory analyses served as reference points and were compared to the average continuous values recorded by the S³ (Ribas-Ribas *et al.*, 2017). This process resulted in the derivation of distinct CFs, which were applied at each depth and during each time interval of the S³ measurements (Ribas-

Con formato: Título 2, Esquema numerado + Nivel: 2 +
Estilo de numeración: 1, 2, 3, ... + Iniciar en: 1 +
Alineación: Izquierda + Alineación: 0.63 cm + Sangría:
1.27 cm

Ribas et al., 2017). Once the salinity values were corrected, the pH was calculated using the CO2Sys program (Version v3.2.0, MATLAB) (Sharp et al., 2020; Van Heuven et al., 2011). These calculated pH_{T25} values were then utilised as reference points for comparison with the average continuous values obtained from the S³ measurements (Ribas-Ribas et al., 2017). After correcting for salinity, the density (ρ) was calculated using the TEOS-10 (<https://www.teos-10.org/index.htm>) equation of state in RStudio (RStudio team, 2023) based on the observed temperature and salinity values. From this calculation, sigma-*t* was defined as the density at a given temperature and salinity minus 1,000 kg m⁻³. The propagated uncertainties for sigma-*t* and pCO₂ were estimated from the measurement precisions of temperature, salinity, pH, DIC, and TA. These estimates provide a quantitative basis for evaluating the reliability of calculated variables in subsequent analyses.

2.3.2.4. Evaporation rate calculation

The evaporation rate (E) (Gill, 1982) was estimated using the following formula, which relates the latent heat flux (Q_E) (Brutsaert, 2013), the latent heat of vaporisation (L_v) (Kittel & Kroemer, 1980), and the calculated density of seawater (ρ):

$$E = \frac{Q_E}{L_v \cdot \rho} \quad (3)$$

2.4.2.5. Statistical Analysis

Since the assumptions of normality and homoscedasticity were not met for the collected data, the Kruskal-Wallis test was chosen as a nonparametric alternative to ANOVA. This test identified significant differences between the data collected during the day and night, revealed significant differences between the data collected during the day and night, as well as between the SML and ULW, and among the medians of the cycles studied. A significance level (α) of 0.05 was established to determine whether the groups differed significantly. All statistical analyses were performed using RStudio (RStudio team, 2023). In addition, to carry out a complete analysis of the variability of the marine carbon system during the study period, the anomalies in temperature, salinity, pH_{T25}, and pCO₂ data were calculated using the following expression: Δ(anomalies in temperature, salinity, pH_{T25}, and pCO₂ data were calculated using the following expression: Δ(SML – ULW). These differences were calculated for diurnal and nocturnal data for each cycle.

3. Results

The primary objective of this study was to understand the global-typical patterns of diurnal variability and depth-related differences in marine biogeochemistry during the observed cycles. Data on Temperature, salinity, pH_{T25}, and pCO₂ were used to perform a statistical analysis of the similarity between the data collected during the diel cycle and to calculate the differences between the values measured in the SML and ULW. Additionally, we examined the temporal distribution using box-and-whisker plots and calculated the air-sea CO₂ exchange across the SML.

3.1. Meteorological conditions

To study the potential variance in the meteorological forcing observed during the observations, time-series graphs were plotted for solar radiation and wind speed (Figure 2Figure 2). A consistent pattern of solar radiation

Con formato: Sin Resaltar

Con formato: Subíndice

Con formato: Subíndice

Con formato: Fuente: Sin Negrita, Sin Cursiva

was observed during all three cycles, with peaks of 525, 404, and 420 W m⁻² observed at 14:00 UTC. Relatively low wind speeds were recorded during the day in all three cycles, averaging 1.26 ± 1.46 m s⁻¹. Maximum wind speeds were observed at 14:00 and 18:00 UTC, higher for Cycles 1 and 2 (2.14 m s⁻¹ and 5.22 m s⁻¹) than during Cycle 3 (0.95 m s⁻¹). Additionally, a decrease in wind speed was observed throughout the night, approaching near-zero values, except during Cycle 3, when the wind speed remained consistently close to zero.

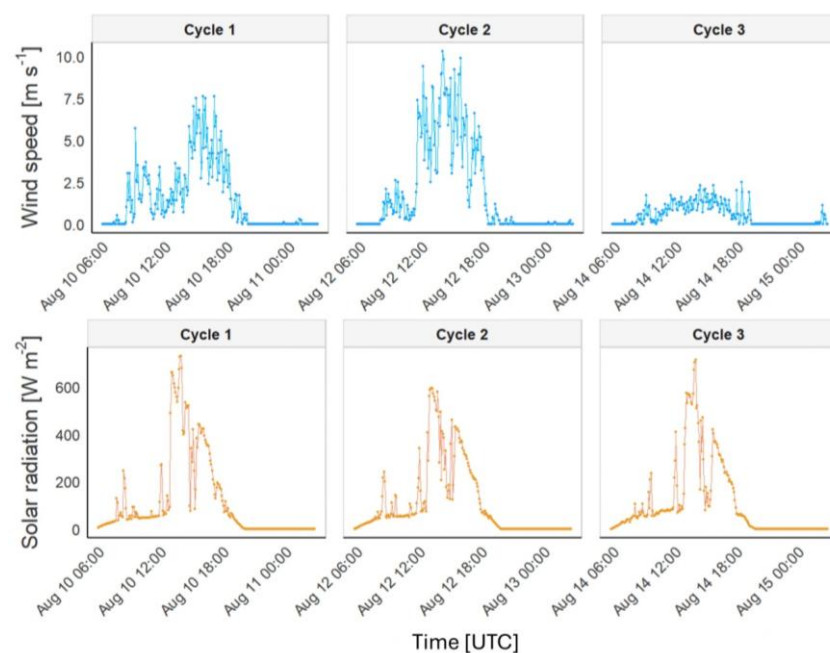


Figure 2. Time series showing wind speed and solar radiation on Zlarin Island (Figure 1) during the three studied cycles.

3.2. Daily trends

To investigate the overall distribution of physicochemical parameters throughout the daily sampling period at the SML and ULW, we show box-and-whisker plots for temperature, salinity, and pH_{T25} across different time intervals (Figure 3). We also performed the Kruskal-Wallis test to determine statistically significant differences (see section 2.5, Materials and Methods) between the SML and ULW (Table S1). The analysis revealed no significant temperature differences between the two depths during Cycle 1 (SML: 25.00 ± 0.85 °C; ULW: 24.90 ± 0.72 °C) and Cycle 2 (SML: 25.40 ± 0.62 °C; ULW: 25.40 ± 0.83 °C). However, in Cycle 3, ULW was slightly warmer, with a mean temperature of 26.60 ± 0.72 °C compared to 26.20 ± 1.20 °C in the SML. For salinity, significant differences were detected between SML and ULW during Cycles 1 and 2, with ULW exhibiting higher salinity levels in Cycle 1 (SML: 38.90 ± 0.32 g kg⁻¹; ULW: 39.10 ± 0.32 g kg⁻¹) and in Cycle 2 (SML: 39.2 ± 0.27 g kg⁻¹; ULW: 39.4 ± 0.29 g kg⁻¹). Notably, the salinity data showed greater variability, especially in Cycle 2, in the SML, whereas the ULW remained relatively constant. The pH_{T25} data collected over

Con formato: Fuente: Sin Negrita, Sin Cursiva

Con formato: Inglés (Estados Unidos)

the three cycles displayed considerable variability, with fluctuations observed throughout the day. The SML and ULW data showed significant differences during the first two cycles, with slightly higher values in the SML for Cycle 1 (SML: 8.030 ± 0.020 ; ULW: 8.020 ± 0.033) and for Cycle 2 (SML: 8.020 ± 0.020 ; ULW: 8.010 ± 0.024). No significant differences were observed in Cycle 3 (SML: 8.020 ± 0.032 ; ULW: 8.020 ± 0.032).

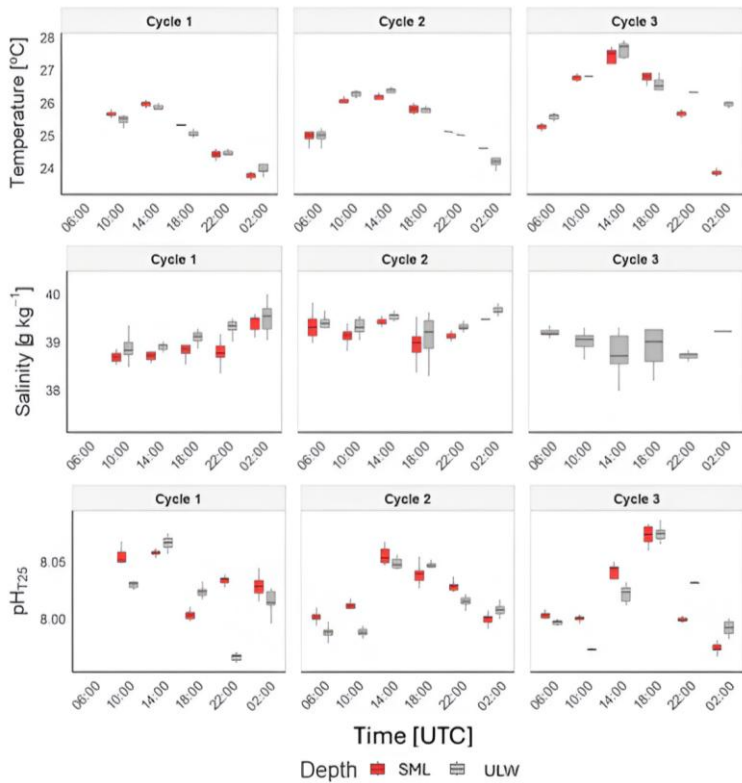


Figure 3. Box-and-whisker plots for the different time steps at which measurements were obtained at both the SML and ULW for temperature, salinity, and $\text{pH}_{\text{T}25}$. Each boxplot represents all measurements obtained during a single 30–45 min deployment (data at 30-minute deployment (data collected at 30-second intervals), with four daytime and two nighttime deployments per cycle. The horizontal line within each box denotes the mean of the data, whereas the vertical line associated with each box represents the 25th and 75th percentiles (Q1 and Q3) of the data.

3.3. Diel variability and depth-related anomalies

To assess diel variability in the marine carbon system, we statistically compared the thermohaline and key carbon cycle variables, $\text{pH}_{\text{T}25}$ and pCO_2 , between day and night in the SML and ULW (Figure 4Figure 4, Table 2Table 4). Additionally, we calculated $\Delta\text{SML-ULW}$ to evaluate the magnitude of vertical anomalies during diurnal and nocturnal conditions. The analysis of thermohaline variables indicated significant differences between diurnal and nocturnal data at the two depths across the three cycles (Table S2). However, the salinity data recorded from ULW during Cycle 3 did not exhibit significant differences. The observed anomalies between

Con formato: Fuente: Sin Negrita, Sin Cursiva, Color de fuente: Automático

Con formato: Fuente: Sin Negrita, Sin Cursiva

the SML and ULW varied across the three cycles for temperature. In Cycle 1, the SML experienced positive diurnal and negative nocturnal temperature anomalies on average (0.19 ± 0.14 ; -0.10 ± 0.14 °C). During Cycle 2, negative diurnal SML anomalies and positive nocturnal anomalies were observed (-0.13 ± 0.12 ; 0.28 ± 0.18 °C). In Cycle 3, diurnal and nocturnal SML negative anomalies were detected at -0.08 ± 0.24 and -1.34 ± 0.77 °C, respectively. Likewise, it was noted that salinity anomalies in SML were negative in Cycles 1 and 2, both for diurnal

$(-0.23 \pm 0.17$; -0.14 ± 0.19 g kg⁻¹) and nocturnal data (-0.29 ± 0.30 ; -0.15 ± 0.29 g kg⁻¹). These results suggest that external factors, may influence thermohaline variables, affecting the pronounced temporal distribution of the diel cycle.

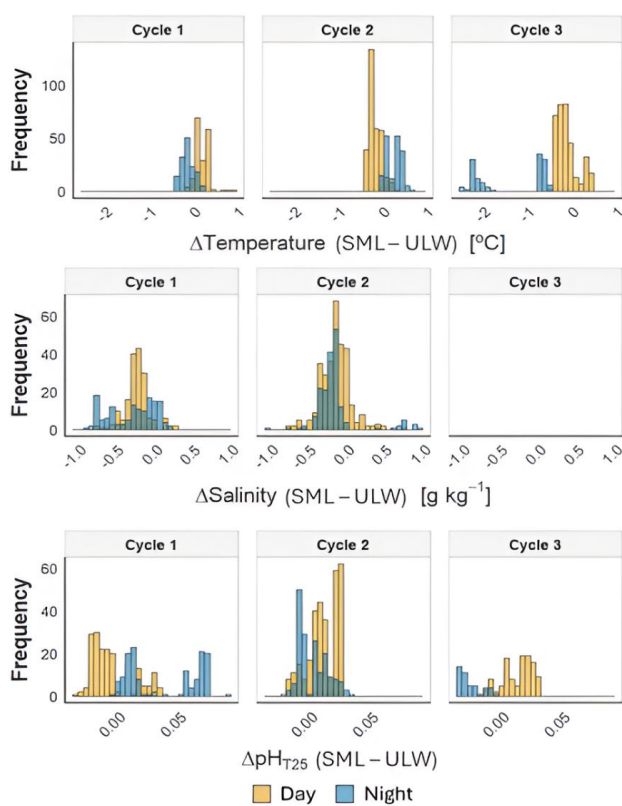


Figure 4. Frequency distribution of the anomaly of temperature, salinity, and pH_{T25} differences between SML and ULW observed during the day (orange) and at night (blue) across the three cycles studied.

When comparing the diurnal and nocturnal data for the variables associated with the marine carbon system at each depth (Table S2), we found significant differences in pH_{T25}, except for the ULW data during Cycle 3. However, no significant differences were observed in the pCO₂ data. The pH_{T25} deltas (Table 2Table 1) revealed that during Cycle 1, lower pH_{T25} values were recorded in the SML for diurnal data and higher for nocturnal data (-0.006 ± 0.018 ; 0.038 ± 0.029). During Cycle 2, the SML showed higher diurnal (0.011 ± 0.012) and lower

Con formato: Fuente: Sin Negrita, Sin Cursiva

nocturnal (-0.002 ± 0.012) pH_{T25} values. Meanwhile, for Cycle 3, the SML indicated higher pH_{T25} values for the diurnal data (0.013 ± 0.012) and lower values for the nocturnal data (0.026 ± 0.009) (Table 2Table 4). For the pCO_2 data during Cycles 1 and 3, lower pCO_2 values were recorded in the SML during both diurnal (-11 ± 56 μatm and -22 ± 22 μatm , respectively) and nocturnal periods (-4 and -8 μatm , respectively) (Table 2Table 4). In Cycle 2, lower diurnal and higher nocturnal values were observed in the SML, with values of -12 ± 19 μatm and 7 μatm , respectively. The large variability between the nighttime and daytime data distributions at the two depths can be attributed to the complex interaction between biological processes and atmospheric and oceanic forcing, such as heat flux and mixing processes.

Table 24. Mean anomalies of temperature, salinity, pH_{T25} , and pCO_2 between the two depths studied ($\Delta(\text{SML-ULW})$).

		Temperature [$^{\circ}\text{C}$]		Salinity [g kg^{-1}]		pH_{T25}		pCO_2 [μatm]	
		n	Δ SML-ULW	n	Δ SML-ULW	n	Δ SML-ULW	n	Δ SML-ULW
Cycle 1	Day	177	0.19 ± 0.14	606	-0.23 ± 0.17	175	-0.006 ± 0.018	3	-11 ± 56
	Night	142	-0.10 ± 0.14	426	-0.29 ± 0.30	140	0.038 ± 0.029	1	-4
Cycle 2	Day	312	-0.13 ± 0.12	972	-0.14 ± 0.19	324	0.011 ± 0.012	4	-12 ± 19
	Night	180	0.28 ± 0.18	559	-0.15 ± 0.29	184	-0.002 ± 0.012	2	7
Cycle 3	Day	365	-0.08 ± 0.24	-	-	141	0.013 ± 0.012	4	-22 ± 22
	Night	132	-1.34 ± 0.77	-	-	53	-0.026 ± 0.009	2	-8

3.4. Biogeochemical processes variability across diel cycles

To assess the variability of biogeochemical processes during the diel cycle, we present time series of temperature, salinity, and pH_{T25} (Figure 5Figure 5). In the time series, large fluctuations were primarily observed in the SML, particularly during the day. This increased variability is consistent with the patterns described in the previous section, although the standard deviations between SML and ULW are similar overall (Table S2). The changes during the day occurred rapidly, with increases and decreases spanning 3- 5-minute intervals for the three parameters. More specifically, during sampling at 18:00 UTC of Cycle 2, we recorded variations over brief intervals, specifically showing changes of approximately 0.28 $^{\circ}\text{C}$ in temperature, 0.30 g kg^{-1} in salinity, and 0.016 units in pH_{T25} . During the night, fluctuations were less frequent and of smaller magnitude, except for a sudden change at the end of the sampling conducted at 02:00 UTC in Cycle 2. At that point, there was a slight increase in pH_{T25} at both SML and ULW, along with a decrease in salinity at both depths. This observation suggests that daytime surface heating, evaporation, and production processes likely result in changes in temperature, salinity, and pH_{T25} , which are less pronounced at night.

Con formato: Fuente: Sin Negrita, Sin Cursiva

Con formato: Fuente: Sin Negrita, Sin Cursiva

Con formato: Fuente: Sin Negrita, Sin Cursiva

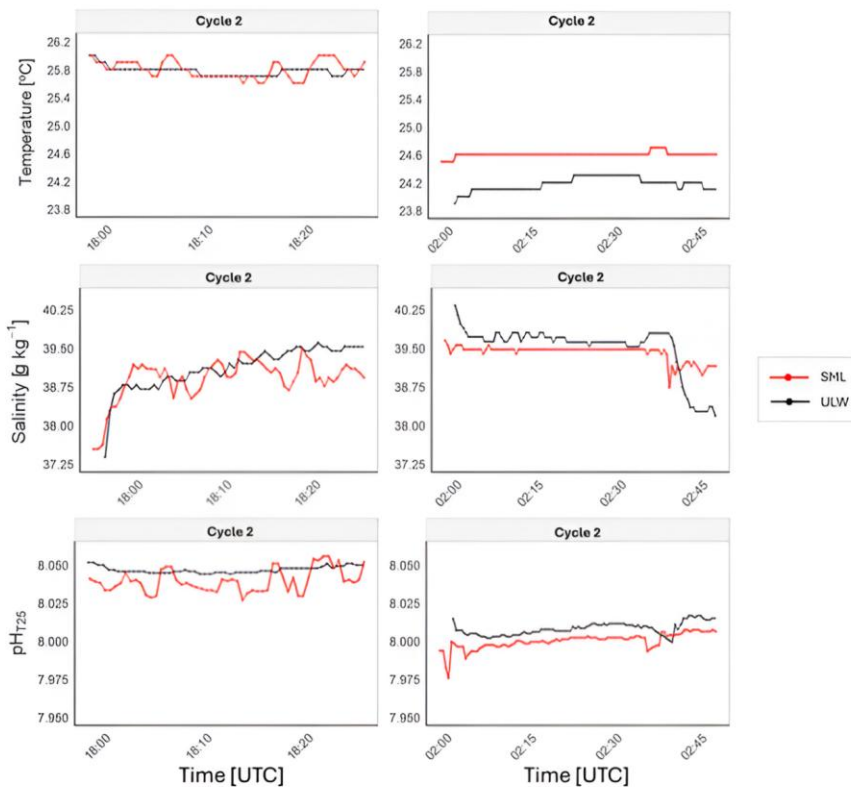


Figure 5. Time series data of temperature, salinity, and pH_{T25} collected during Cycle 2: Diurnal (18:00 UTC, August 12) and Nocturnal (02:00 UTC, August 13) measurements.

To assess the variability observed in the SML, the sigma-*t* time series for Cycle 2 at 18:00 UTC and 02:00 UTC was plotted (Figure 6), and evaporation rates within the SML were calculated for Cycles 1 and 2 (Table 3), as salinity data required for calculations in Cycle 3 were not available. The sigma-*t* time series throughout the day exhibits greater variability in the SML compared to nocturnal data, when the density fluctuation decreased. However, this variability trend of variability was not observed in the ULW. The observed patterns of temperature, salinity, pH_{T25}, and sigma-*t* align with the calculated evaporation rates. In Cycles 1 and 2, the evaporation rates peaked at 14:00 UTC (0.043 mm h⁻¹ and 0.074 mm h⁻¹, respectively). They remained high during the late afternoon at 18:00 UTC (0.042 mm h⁻¹ and 0.041 mm h⁻¹, respectively), coinciding with the periods of highest solar radiation and wind speed (Figure 2). In contrast, the evaporation rate was close to zero at night. This behaviour highlights the influence of meteorological forcing on the SML during the day, highlighting the connection between evaporation and the variability observed, underscoring the connection between evaporation and the observed variability.

Con formato: Fuente: Sin Negrita, Sin Cursiva

Con formato: Fuente: Sin Negrita, Sin Cursiva

Con formato: Fuente: Sin Negrita, Sin Cursiva, Color de fuente: Automático

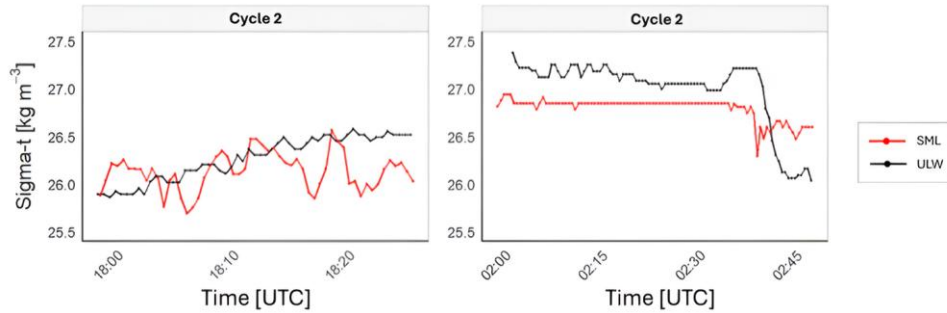


Figure 6. Time series during Cycle 2 for diurnal (18:00 UTC on August 12) and nocturnal (02:00 UTC on August 13) sigma-t data. Sigma-t is defined as the density at a given temperature and salinity minus 1,000 kg m⁻³.

Table 32. Estimated evaporation rates (mm h⁻¹) based on latent heat flux and seawater density in the SML.

Evaporation rates [mm h ⁻¹]				
Cycle	Time (UTC)	Mean	sd	n
Cycle 1	06:00			
	10:00	0.031	$1.261 \cdot 10^{-3}$	41
	14:00	0.043	$4.646 \cdot 10^{-4}$	67
	18:00	0.042	$6.674 \cdot 10^{-4}$	64
	22:00	0.000	0.00	66
	02:00	0.000	0.00	76
Cycle 2	06:00	0.000	0.00	68
	10:00	0.012	$2.040 \cdot 10^{-4}$	111
	14:00	0.074	$1.667 \cdot 10^{-3}$	78
	18:00	0.041	$8.670 \cdot 10^{-4}$	55
	22:00	0.000	0.00	82
	02:00	0.000	$3.960 \cdot 10^{-6}$	98

To study the gas exchange between the atmosphere and the ocean, we calculated the CO₂ fluxes and k values using a wind-based parameterisation (Wanninkhof, 2014) for all three cycles and during both day and night (Figure 7). In Cycle 1, despite the limited incomplete data, a flux of 3.64 ± 1.15 mmol cm⁻² h⁻¹ was detected during the day, while the flux was close to zero at night. A similar pattern appeared in Cycles 2 and 3, where the fluxes peaked at approximately 14:00 UTC and declined to near zero thereafter. However, the mean flux was higher in Cycle 2 (2.04 ± 3.18 mmol cm⁻² h⁻¹) than in Cycle 3 (0.21 ± 0.28 mmol cm⁻² h⁻¹), consistent

Con formato: Fuente: Sin Negrita, Sin Cursiva

with stronger winds. The average wind speeds during the day were 1.5, 1.9, and 0.4 m s⁻¹ for each cycle, respectively, while at night, winds dropped to nearly 0 m s⁻¹ in the three cycles. The *k* values during the day were 1.12 ± 0.15, 2.22 ± 3.31, and 0.09 ± 0.11 cm h⁻¹, whereas at night, they were close to 0 cm h⁻¹. In this context, excluding nocturnal fluxes in the daily average calculations introduced local percentage errors of 33%, 50%, and 43% for Cycles 1, 2, and 3, respectively. The increased daytime wind speeds enhanced CO₂ fluxes, whereas calm nighttime conditions were associated with reduced or nearly zero gas transfer velocities.

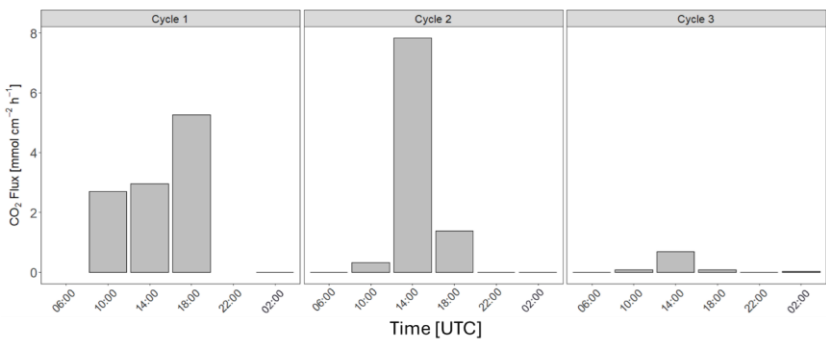


Figure 7. CO₂ fluxes between the atmosphere and the ocean during the studied cycles.

4. Discussion

This study revealed high variability in the SML and ULW during the diel cycle, with significant differences ($p < 0.05$) in temperature, salinity, and pH_{T25} when comparing diurnal and nocturnal data at both depths (Table S1). These results highlight the differences between the meteorological forces that influence the physicochemical properties of seawater during the day and night. For example, during the day, the combined forcing of solar radiation and increased wind speed enhances evaporation rates (Table 3Table 2), resulting in the cooling of the SML (Gassen *et al.*, 2023), which drives short-term changes not only in temperature and salinity but also in this causing changes in temperature, salinity, and pH_{T25} (Figure 4Figure 4). This response reflects both the temperature dependence of carbonate speciation (Zeebe & Wolf-Gladrow, 2001). In addition, it is influenced by the combined effect of evaporation, which tends to increase salinity, alkalinity and thus pH_{T25}, and vertical mixing, which can dilute this signal by introducing water with lower pH_{T25} and higher pCO₂. This means that the SML is subjected to short-term short-term fluctuations that coincide with changes in wind speed. These fluctuations directly influence thermohaline features, CO₂ system parameters (Acuña *et al.*, 2008), and the kinetics of the metabolic processes occurring in the marine environment (Nimick *et al.*, 2011). Accordingly, in response to the solar photocycle, many marine biogeochemical processes operate on a 24-hour cycle (Nimick *et al.*, 2011), with daily variations comparable in magnitude to the annual variations associated with the amount of solar radiation reaching the ocean surface at different times of the year (Herring *et al.*, 1990; Nimick *et al.*, 2011).

Con formato: Fuente: Sin Negrita, Sin Cursiva

Con formato: Fuente: Sin Negrita, Sin Cursiva

Con formato: Sin Resaltar

Con formato: Subíndice

Con formato: Subíndice

Con formato: Fuente: Cursiva

Con formato: Resaltar

Regarding the variability observed during the day and night, we detected differences in the diurnal temperature data, reaching up to +1.89 °C in the SML and +1.36 °C in the ULW. The calculated mean temperature values correspond to the Middle Adriatic Surface Water mass (Table S1). Previous studies have reported mean summertime temperatures in the SML of 25.1 °C (Frka *et al.*, 2009) and 27.4 ± 2.9 °C (Milinković *et al.*, 2022). Interestingly, the negative diurnal SML anomalies in Cycles 2 and 3 differ from the typical ~~low-wind patterns~~ *warming pattern in low wind conditions* (Wurl *et al.*, 2019), suggesting that ~~localized~~ *localised* mixing or evaporative cooling may have offset surface warming. *In our study, strong stratification combined with weak winds likely promoted localised evaporative cooling and convection, offsetting the expected surface warming, as described in previous studies of near-surface instabilities* (Cronin & Sprintall, 2001; Soloviev & Lukas, 2014). Similarly, the observed negative salinity anomaly in the SML could also be linked to these processes. While evaporation driven by intense solar radiation tends to increase salinity in the SML (Frka *et al.*, 2009; Wurl *et al.*, 2019), the consistently negative salinity anomalies observed in Cycles 1 and 2 (Table 2) ~~Table 4~~ suggest *active* vertical mixing, *most likely associated with convective processes*. This explains the daily variability in salinity distribution between the SML and ULW, with mean values of 39.09 ± 0.33 g kg⁻¹ and 39.15 ± 0.34 g kg⁻¹, respectively.

In this context, the contribution of external forcing factors, such as river discharge, precipitation, and tides, to the observed diurnal variability appears to be minimal. The ~~The~~ Krka River has the highest outflow rates in the region, but it ~~usually has lower discharge in~~ *typically experiences lower discharge in the during the summer*. *This seasonal decrease in freshwater input contributes to the higher salinity values observed in both the SML and ULW compared to periods of stronger river discharge* ~~months, which contributes to the increased salinity observed in the SML and ULW~~ (Frka *et al.*, 2009; Marcinek *et al.*, 2020). ~~During dry periods, submarine groundwater discharge is also minor~~ *contributes only a small amount*, between 0.19-0.31 m³ s⁻¹ *during dry periods* (Liu *et al.*, 2019), compared to its annual mean of 52.9 m³ s⁻¹ (Bužančić *et al.*, 2016; Marcinek *et al.*, 2020). *In addition, precipitation during the first half of August 2020 was very low, averaging 1.4 mm (2020; Croatian Meteorological and Hydrological Service, 2020), further limiting freshwater input and variability in river flow. Similarly, tidal effects at this location are minimal, characterized by a microtidal range of 0.2 to 0.5 meters (Cukrov, 2024). Given the stable stratification of the estuary, such small tidal amplitudes are insufficient to generate significant tidally driven vertical mixing. Instead, the variability observed can be explained by localised* ~~observed variability can be explained by localized~~ *near-surface mixing linked to evaporation, density instabilities, and short-term turbulence at the air-sea interface. Furthermore, the observed variability follows a diurnal (24-hour) cycle rather than a semi-diurnal (12-hour) cycle, reinforcing the interpretation that the patterns are primarily driven by surface warming and evaporation rather than tidal forcing* (Wurl *et al.*, 2019). This contrasts with mesotidal environments (e.g., Stolle *et al.*, 2020), where tidal mixing complicates the detection of diurnal variability, highlighting the advantage of studying these processes in microtidal settings such as the Adriatic.

The interaction between biological processes and the physicochemical properties of seawater is complex (Álvarez *et al.*, 2014; Cantoni *et al.*, 2012) and has a delicate balance in the marine environment (Cantoni *et al.*, 2012; Takahashi *et al.*, 2002). This interaction directly influences biogeochemical processes typically regulated by production and respiration (Poulson & Sullivan, 2010). These processes significantly affect the pH of

Con formato: Fuente: Sin Negrita

Con formato: Fuente: Sin Negrita, Sin Cursiva

Con formato: Fuente: Sin Negrita

Con formato: Sin Resaltar

seawater through the uptake or removal of CO₂. During the day, photosynthesis lowers pCO₂ levels and increases pH by consuming CO₂, whereas at night, CO₂ from respiration accumulates, increasing pCO₂ and decreasing pH (Cantoni *et al.*, 2012). However, as we can see in Cycle 3 (Table S2), the observed increase in pCO₂ (525 ± 47 µatm) and pH_{T25} (8.042 ± 0.020) values during the day compared to those measured at night (465 µatm; 7.993 ± 0.026). This pattern likely reflects biological and mixing dynamics: may be linked to several processes enhanced, including increased respiration and CO₂ accumulation in the upper layers of the water due to limited mixing may offset the anticipated photosynthetic uptake (Takahashi *et al.*, 2002), while various environmental factors that may offset the anticipated effects of photosynthesis or the possibility of photoinhibition caused by excessive under solar radiation (Feng *et al.*, 2008; Platt *et al.*, 1980) could reduce photosynthesis efficiency. Taken together, these processes provide a plausible explanation for the unexpected daytime increase in pCO₂ despite favorable/favourable light conditions (Takahashi *et al.*, 2002), and an accumulation of CO₂ in the upper layers of the water due to limited mixing (Takahashi *et al.*, 2002).

Con formato: Fuente: Cursiva

The complexity of the coupled thermohaline and pH dynamics in seawater is highlighted in the time-series results (Figure 5). The observed fluctuations in the SML for temperature, salinity, and pH_{T25} may be due to buoyancy fluxes. Wind, thermohaline fluctuations, precipitation, and evaporation significantly influence the have a significant influence on surface turbulence (Cronin & Sprintall, 2001). The SML absorbs heat from sunlight and cools through radiation and heat loss, leading to changes in temperature and salinity that disrupt buoyancy, cause convective overturning, entrain deeper water from the ULW, and eventually promote mixing (Cronin & Sprintall, 2001). Wind can also enhance this process by creating tangential stress that acts as a vertical momentum flux. Temperature and salinity changes in the SML led to stratification or convection with mixing (Figure 5), depending on oceanic and atmospheric forcing, with mixing, depending on oceanic and atmospheric forcing (Figure 5). This process has already been observed in the SML (Wurl *et al.*, 2019) and was found to regulate buoyancy fluxes through evaporative salinisation, playing a crucial role in the exchange of climate-relevant gases and heat between the ocean and the atmosphere.

In this context, the existence of these buoyancy fluxes only during the day could also explain the diel difference in CO₂ exchange between the atmosphere and the ocean. As observed in this study, the CO₂ fluxes exhibited differences between daytime (1.948 ± 2.4552 mmol cm⁻² h⁻¹) and nighttime (0.01 ± 0.012 mmol cm⁻² h⁻¹) conditions. This pattern is consistent with the strong dependence of the gas transfer velocity (k) on wind forcing (Wanninkhof, 2014), confirming that wind is the dominant driver of diel variability. In addition, thus, during the day, daytime buoyancy fluxes, enhanced by wind-driven evaporation and density instabilities, may further facilitate CO₂ exchange during the day, amplifying the effect of wind facilitate the exchange of CO₂ between the two compartments, accounting for a higher flux than at night. Additionally, the absence of wind at night reduced the calculated flux to nearly zero. This observation is consistent with previous suggestions suggesting that gas transfer velocity parameterisations without an intercept may underestimate very calm conditions in very calm waters not be appropriate (Ribas-Ribas *et al.*, 2019). Other processes, such as small-scale convection or vertical pCO₂ gradients in the upper water column (Liss & Merlivat, 1986; Stolle *et al.*, 2020), may also modulate short-term variability, but their contribution in our dataset appears minor compared to wind forcing. At the same time, SML properties themselves may contribute: slightly lower temperature and salinity enhance CO₂ solubility, while reduced turbulence at the boundary layer further limits exchange. Moreover, even without wind,

Con formato: Color de fuente: Negro

Con formato: Color de fuente: Automático

Con formato: Fuente: Sin Negrita

Con formato: Fuente: Sin Negrita

Con formato: Fuente: Sin Negrita

convective airflow driven by temperature gradients can facilitate gas exchange between the surface and atmosphere (Liss & Merlivat, 1986). This study's diel variability aligns with other research findings, suggesting that another main factor affecting this difference is the vertical $p\text{CO}_2$ gradient in the upper water column, potentially affecting gas transfer estimates (Stolle *et al.*, 2020). Therefore, neglecting nocturnal fluxes may result in overestimation, as in this study, where the three cycles were overvalued by 33%, 50%, and 44%, respectively. The main implication of our results is that neglecting nocturnal fluxes leads to a systematic bias: the three diel cycles were overestimated by 33%, 50%, and 44%, respectively. Thus, while wind remains the principal driver, including nighttime measurements is essential to avoid biased daily estimates.

5. Conclusions

This study observed a clear diel variability in the distribution of thermohaline features and variables describing the marine inorganic carbon cycle, including temperature, salinity, $\text{pH}_{\text{T}25}$, and $p\text{CO}_2$. The SML experiences pronounced fluctuations in these parameters throughout the day, influenced by daily changes, like solar radiation, which directly affect the described variables and the environment's metabolic activity. In addition, higher CO_2 fluxes were observed during the day, coinciding with increased wind speeds and buoyancy fluxes that enhanced the CO_2 exchange between the two compartments. Thus, by emphasising the study of diel cycles, it has been observed that the daily variability of biogeochemical processes is in a delicate balance, making it challenging to obtain a comprehensive global understanding of marine chemistry. Technological advances have been made in sampling equipment for short temporal and spatial scales in recent decades. However, such progress has not been extended to nighttime observations, which remain significantly more challenging due to greater logistical complexity and heightened safety considerations when operating aboard oceanographic vessels at night. In this context, it is essential to study complete diel cycles, which are crucial for understanding the global carbon budget and its associated uncertainties. Thus, generating a network of diurnal cycle data will identify the drivers of changes in marine chemistry, allowing for assessing the assessment of the responses of marine ecosystems in the context of climate change.

Data Availability Statements

The datasets supporting the findings of this study are available at PANGAEA. The diel variability dataset is accessible at <https://doi.pangaea.de/10.1594/PANGAEA.984017> (Ribas-Ribas *et al.*, 2023a). Additional supporting datasets include meteorological data (<https://doi.pangaea.de/10.1594/PANGAEA.984331>; Ribas-Ribas *et al.*, 2023b), discrete bottle samples (<https://doi.pangaea.de/10.1594/PANGAEA.984018>; Ribas-Ribas *et al.*, 2023c), and high-frequency measurements (<https://doi.pangaea.de/10.1594/PANGAEA.984020>; Ribas-Ribas *et al.*, 2023d). The data supporting the findings of this study have been submitted to PANGAEA and are currently undergoing curation and DOI assignment. In the meantime, the data are available for review and use at [\[cloud link\]](#).

Con formato: Inglés (Estados Unidos)

Acknowledgements

This work was funded by the German Research Foundation (DFG), project number 427614800, and by the Croatian Science Foundation under the project IP-2018-01-3105: *Biochemical Responses of Oligotrophic Adriatic Surface Ecosystems to Atmospheric Deposition Inputs* (BiREADI). It was also supported by the German Academic Exchange Service (DAAD) under project 57513644: *Diurnal Dynamics at the Sea-Atmosphere Interface (INSIST)*. Additionally, the author gratefully acknowledges the support from the Erasmus+ KA 131 SMP OUT program (2022-2023) for funding a research internship at the Carl von Ossietzky Universität Oldenburg - Institut für Chemie und Biologie des Meeres (ICBM). The authors thank Carola Lehnert, Brandy T. Robinson, and Lisa Gassen for operating the sea surface scanner and conducting SML sampling, Carmen Cöhr for initial S³ data treatment, and Leonie Jaeger for assistance with the evaporation rate calculations.

Author Contribution

AL-P: Data Curation, Formal Analysis, Methodology, Visualization, Writing – Original Draft, Writing – Review & Editing. **OW:** Funding Acquisition, Resources, Formal Analysis, Writing – Review & Editing. **SF:** Funding Acquisition, Resources, Formal Analysis, Writing – Review & Editing. **MR-R:** Conceptualisation, Formal Analysis, Visualization, Funding Acquisition, Resources, Supervision, Writing – Original Draft, Writing – Review & Editing.

References

- Acuña, V., Wolf, A., Uehlinger, U., and Tockner, K.: Temperature dependence of stream benthic respiration in an alpine river network under global warming, *Freshw. Biol.*, 53, 2076–2088, <https://doi.org/10.1111/j.1365-2427.2008.02028.x>, 2008.
- Álvarez, M., Sanleón-Bartolomé, H., Tanhua, T., Mintrop, L., Luchetta, A., Cantoni, C., Schroeder, K., and Civitarese, G.: The CO₂ system in the Mediterranean Sea: a basin-wide perspective, *Ocean Sci.*, 10, 69–92, <https://doi.org/10.5194/os-10-69-2014>, 2014.
- Álvarez-Rodríguez, M.: The CO₂ system observations in the Mediterranean Sea: past, present and future, in: Designing Med-SHIP: a program for repeated oceanographic surveys, CIESM Workshop Monographs, No. 43, edited by: Briand, F., CIESM, Monaco, pp. 41–50, <https://ciesm.org/catalog/index.php?article=1043>, 2012.
- Bergamasco, A., and Malanotte-Rizzoli, P.: The circulation of the Mediterranean Sea: a historical review of experimental investigations, *Adv. Oceanogr. Limnol.*, 1, 11–28, <https://doi.org/10.1080/19475721.2010.491656>, 2010.

520 Borges, A. V.: Do we have enough pieces of the jigsaw to integrate CO₂ fluxes in the coastal ocean?, *Estuaries*,
28, 3–27, <https://doi.org/10.1007/BF02732750>, 2005.

~~Brutsaert, W.: Evaporation into the Atmosphere: Theory, History and Applications, Environmental Fluid
Mechanics, Springer, Dordrecht, Netherlands, 302 pp., <https://doi.org/10.1007/978-94-017-1497-6>,
2013.~~

525 Bužančić, M., Gladan, Ž. N., Marasović, I., Kušpilić, G., and Grbec, B.: Eutrophication influence on
phytoplankton community composition in three bays on the eastern Adriatic coast, *Oceanologia*, 58,
302–316, <https://doi.org/10.1016/j.oceano.2016.05.003>, 2016.

Cantoni, C., Luchetta, A., Celio, M., Cozzi, S., Raicich, F., and Catalano, G.: Carbonate system variability in the
Gulf of Trieste (North Adriatic Sea), *Estuarine, Coastal Shelf Sci.*, 115, 51–62,
530 <https://doi.org/10.1016/j.ecss.2012.07.006>, 2012.

Cantoni, C., Luchetta, A., Chiggiato, J., Cozzi, S., Schroeder, K., and Langone, L.: Dense water flow and
carbonate system in the southern Adriatic: A focus on the 2012 event, *Mar. Geol.*, 375, 15–27,
<https://doi.org/10.1016/j.margeo.2015.08.013>, 2016.

~~Croatian Meteorological and Hydrological Service.:Precipitation data for August 2020, available at:
535 <https://meteo.hr>, 2020.~~

Cronin, M. F., and Sprintall, J.: Wind-and buoyancy-forced upper ocean, in: *Elements of Physical
Oceanography: A Derivative of the Encyclopedia of Ocean Sciences*, 237–245,
<https://doi.org/10.1006/rwos.2001.0157>, 2001.

~~Cukrov, N., Cindrić, A.-M., Omanović, D., & Cukrov, N.: Spatial distribution, ecological risk assessment, and
source identification of metals in sediments of the Krka River Estuary (Croatia), *Sustainability*, 16, 1800,
540 <https://doi.org/10.3390/su16051800>, 2024a.~~

~~Cukrov, N., Cukrov, N., & Omanović, D.: Early diagenetic processes in the sediments of the Krka River Estuary,
J. Mar. Sci. Eng., 12, 466, <https://doi.org/10.3390/jmse12030466>, 2024b.▲~~

Cunliffe, M., Engel, A., Frka, S., Gašparović, B., Guitart, C., Murrell, J. C., Salter, M., Stolle, C., Upstill-
545 Goddard, R., and Wurl, O.: Sea surface microlayers: A unified physicochemical and biological
perspective of the air–ocean interface, *Prog. Oceanogr.*, 109, 104–116,
<https://doi.org/10.1016/j.poccean.2012.08.004>, 2013.

De Montety, V., Martin, J. B., Cohen, M. J., Foster, C., and Kurz, M. J.: Influence of diel biogeochemical cycles
on carbonate equilibrium in a karst river, *Chem. Geol.*, 283(1–2), 31–43,
550 <https://doi.org/10.1016/j.chemgeo.2010.12.025>, 2011.

Con formato: Normal

Con formato: Normal

Con formato: Color de fuente: Automático

Dickson, A. G., and Millero, F. J.: A comparison of the equilibrium constants for the dissociation of carbonic acid in seawater media, *Deep Sea Res. Part A*, 34(10), 1733–1743, [https://doi.org/10.1016/0198-0149\(87\)90021-5](https://doi.org/10.1016/0198-0149(87)90021-5), 1987.

Dickson, A. G., Sabine, C. L., and Christian, J. R. (Eds.): Guide to best practices for ocean CO₂ measurements, PICES Special Publication 3, North Pacific Marine Science Organization, 191 pp., ISBN 1-897176-07-4, 2007.

Doney, S. C., Fabry, V. J., Feely, R. A., and Kleypas, J. A.: Ocean Acidification: The Other CO₂ Problem, *Annu. Rev. Mar. Sci.*, 1(1), 169–192, <https://doi.org/10.1146/annurev.marine.010908.163834>, 2009.

Engel, A., Bange, H. W., Cunliffe, M., Burrows, S. M., Friedrichs, G., Galgani, L., Herrmann, H., Hertkorn, N., Johnson, M., Liss, P. S., Quinn, P. K., Schartau, M., Soloviev, A., Stolle, C., Upstill-Goddard, R. C., Van Pinxteren, M., & Zäncker, B.: The ocean's vital skin: toward an integrated understanding of the sea surface microlayer, *Front. Mar. Sci.*, 4, 165, <https://doi.org/10.3389/fmars.2017.00165>, 2017.

Fanning, K. A., and Pilson, M.: On the Spectrophotometric determination of dissolved silica in natural waters, *Anal. Chem.*, 45(1), 136–140, <https://doi.org/10.1021/ac60323a021>, 1973.

Feng, Y., Warner, M. E., Zhang, Y., Sun, J., Fu, F.-X., Rose, J. M., and Hutchins, D. A.: Interactive effects of increased pCO₂, temperature and irradiance on the marine coccolithophore *Emiliania huxleyi* (Prymnesiophyceae), *Eur. J. Phycol.*, 43(1), 87–98, <https://doi.org/10.1080/09670260701664674>, 2008.

Friedlingstein, P., O'Sullivan, M., Jones, M. W., Andrew, R. M., Hauck, J., Landschützer, P., Le Quéré, C., Li, H., Luijkx, I. T., and Olsen, A.: Global carbon budget 2024, *Earth Syst. Sci. Data*, 17, 965–1098, <https://doi.org/10.5194/essd-17-965-2025>, 2024.

Frka, S., Kozarac, Z., and Čosović, B.: Characterization and seasonal variations of surface active substances in the natural sea surface micro-layers of the coastal Middle Adriatic stations, *Estuar. Coast. Shelf Sci.*, 85(4), 555–564, <https://doi.org/10.1016/j.ecss.2009.09.023>, 2009.

Garbe, C. S., Rutgersson, A., Boutin, J., De Leeuw, G., Delille, B., Fairall, C. W., Gruber, N., Hare, J., Ho, D. T., Johnson, M. T., Nightingale, P. D., Pettersson, H., Piskozub, J., Sahlée, E., Tsai, W., Ward, B., Woolf, D. K., & Zappa, C. J.: Transfer across the air–sea interface, in: *Ocean–Atmosphere Interactions of Gases and Particles*, edited by: Liss, P. S. and Johnson, M. T., Springer, Berlin, Heidelberg, Germany, 55–112, https://doi.org/10.1007/978-3-642-25643-1_2, 2014.

Gassen, L., Badewien, T. H., Ewald, J., Ribas-Ribas, M., and Wurl, O.: Temperature and Salinity Anomalies in the Sea Surface Microlayer of the South Pacific during Precipitation Events, *J. Geophys. Res. Oceans*, e2023JC019638, <https://doi.org/10.1029/2023JC019638>, 2023.

Con formato: Normal

Con formato: Normal

Con formato: Normal

Gattuso, J.-P., Allemand, D., & Frankignoulle, M.: Photosynthesis and calcification at cellular, organismal and community levels in coral reefs: a review on interactions and control by carbonate chemistry, *Am. Zool.*, 39, 160–183, <https://doi.org/10.1093/icb/39.1.160>, 1999.

Gattuso, J.-P., Magnan, A., Billé, R., Cheung, W. W. L., Howes, E. L., Joos, F., ... and Turley, C.: Contrasting futures for ocean and society from different anthropogenic CO₂ emissions scenarios, *Science*, 349(6243), aac4722, <https://doi.org/10.1126/science.aac4722>, 2015.

~~Gill, A. E.: Atmosphere-Ocean Dynamics, Academic Press, ISBN 0-12-283520-4, 1982.~~

Hassoun, A. E. R., Bantelman, A., Canu, D., Comeau, S., Galdies, C., Gattuso, J.-P., Giani, M., Grelaud, M., Hendriks, I. E., Ibello, V., Idrissi, M., Krasakopoulou, E., Shaltout, N., Solidoro, C., Swarzenski, P. W., & Ziveri, P.: Ocean acidification research in the Mediterranean Sea: Status, trends and next steps, *Front. Mar. Sci.*, 9, 892670, <https://doi.org/10.3389/fmars.2022.892670>, 2022.

Hassoun, A. E. R., Gemayel, E., Krasakopoulou, E., Goyet, C., Abboud-Abi Saab, M., Guglielmi, V., Touratier, F., & Falco, C.: Acidification of the Mediterranean Sea from anthropogenic carbon penetration, *Deep Sea Res. Part I*, 102, 1–15, <https://doi.org/10.1016/j.dsr.2015.04.005>, 2015.

Herring, P. J., Campbell, A. K., Whitfield, M., and Maddock, L. (Eds.): *Light and Life in the Sea*, Cambridge University Press, Cambridge, UK, 366 pp., ISBN 978-0521392075, 1990.

Hoegh-Guldberg, O., Cai, R., Poloczanska, E. S., Brewer, P. G., Sundby, S., Hilmi, K., Fabry, V. J., and Jung, S.: The ocean, in: *Climate Change 2014: Impacts, Adaptation, and Vulnerability. Part B: Regional Aspects*, edited by: Barros, V. R., Field, C. B., Dokken, D. J., Mastrandrea, M. D., Mach, K. J., Bilir, T. E., Chatterjee, M., Ebi, K. L., Estrada, Y. O., Genova, R. C., Girma, B., Kissel, E. S., Levy, A. N., MacCracken, S., Mastrandrea, P. R., and White, L. L., Cambridge University Press, Cambridge, United Kingdom and New York, NY, USA, 1655–1731, <https://doi.org/10.1017/CBO9781107415386.026>, 2014.

Humphreys, M. P., Lewis, E. R., Sharp, J. D., and Pierrot, D.: PyCO2SYS v1.8: Marine carbonate system calculations in Python, *Geoscientific Model Development*, 15(1), 15–43, <https://doi.org/10.5194/gmd-15-15-2022>, 2022.

Kittel, C., and Kroemer, H.: *Thermal Physics*, Macmillan, ISBN 978-0716710882, 1980.

~~Lan, X., Tans, P., Thoning, K., and NOAA Global Monitoring Laboratory: Trends in globally-averaged CO₂ determined from NOAA Global Monitoring Laboratory measurements, NOAA GML [data set], <https://doi.org/10.15138/9N0H-ZH07>, 2023.~~

Con formato: Normal

Con formato: Normal

- Laskov, C., Herzog, C., Lewandowski, J., and Hupfer, M.: Miniaturized photometrical methods for the rapid
 615 analysis of phosphate, ammonium, ferrous iron, and sulfate in pore water of freshwater sediments,
Limnol. Oceanogr. Methods, 5, 63–71, <https://doi.org/10.4319/lom.2007.5.63>, 2007.
- Lee, K., Kim, T.-W., Byrne, R. H., Millero, F. J., Feely, R. A., and Liu, Y.-M.: The universal ratio of boron to
 chlorinity for the North Pacific and North Atlantic oceans, *Geochim. Cosmochim. Acta*, 74, 1801–1811,
<https://doi.org/10.1016/j.gca.2009.12.027>, 2010.
- 620 Liss, P. S., and Duce, R. A. (Eds.): *The Sea Surface and Global Change*, Cambridge University Press, ISBN
 9780521562737, 1997.
- Liss, P. S., and Merlivat, L.: Air–sea gas exchange rates: introduction and synthesis, in: *The Role of Air–Sea
 Exchange in Geochemical Cycling*, edited by: Buat-Ménard, P., Springer, Dordrecht, Netherlands, 113–
 127, https://doi.org/10.1007/978-94-009-4738-2_5, 1986.
- 625 Liu, J., Hrutić, E., Du, J., Gašparović, B., Čanković, M., Cukrov, N., Zhu, Z., and Zhang, R.: Net submarine
 groundwater-derived dissolved inorganic nutrients and carbon input to the oligotrophic stratified karstic
 estuary of the Krka River (Adriatic Sea, Croatia), *J. Geophys. Res.-Oceans*, 124, 4334–4349,
<https://doi.org/10.1029/2018JC014814>, 2019.
- Marcinek, S., Santinelli, C., Cindrić, A.-M., Evangelista, V., Gonnelli, M., Layglon, N., Mounier, S., Lenoble, V.,
 630 and Omanović, D.: Dissolved organic matter dynamics in the pristine Krka River estuary (Croatia),
Mar. Chem., 225, 103848, <https://doi.org/10.1016/j.marchem.2020.103848>, 2020.
- Mehrbach, C., Culbertson, C. H., Hawley, J. E., and Pytkowicz, R. M.: Measurement of the apparent dissociation
 constants of carbonic acid in seawater at atmospheric pressure 1, *Limnol. Oceanogr.*, 18, 897–907,
<https://doi.org/10.4319/lo.1973.18.6.0897>, 1973.
- 635 Milinković, A., Penezić, A., Kušan, A. C., Gluščić, V., Žužul, S., Skejić, S., Šantić, D., Godec, R., Pehnec, G.,
 Omanović, D., Engel, A., and Frka, S.: Variabilities of biochemical properties of the sea surface
 microlayer: Insights to the atmospheric deposition impacts, *Sci. Total Environ.*, 838, 156440,
<https://doi.org/10.1016/j.scitotenv.2022.156440>, 2022.
- Nimick, D. A., Gammons, C. H., and Parker, S. R.: Diel biogeochemical processes and their effect on the
 640 aqueous chemistry of streams: A review, *Chem. Geol.*, 283, 3–17,
<https://doi.org/10.1016/j.chemgeo.2010.08.017>, 2011.

Orr, J. C., Fabry, V. J., Aumont, O., Bopp, L., Doney, S. C., Feely, R. A., Gnanadesikan, A., Gruber, N., Ishida,
A., Joos, F., Key, R. M., Lindsay, K., Maier-Reimer, E., Matear, R., Monfray, P., Mouchet, A., Najjar, R. G.,
Plattner, G.-K., Rodgers, K. B., Sabine, C. L., Sarmiento, J. L., Schlitzer, R., Slater, R. D., Totterdell, I. J.,

645 [Weirig, M.-F., Yamanaka, Y., and Yool, A.: Anthropogenic ocean acidification over the twenty-first century and its impact on calcifying organisms, *Nature*, 437, 681–686, <https://doi.org/10.1038/nature04095>, 2005.](#)

650 [Pecci, M., di Sarra, A., Sferlazzo, D., Anello, F., Di Iorio, T., Colella, S., Iaccarino, A., Marullo, S., Meloni, D., Monteleone, F., Pace, G., & Piacentino, S.: Ocean–atmosphere CO₂ flux at the Lampedusa Oceanographic Observatory, available at: \[https://www.lampedusa.enea.it/dataaccess/ocean_co2fluxes\]\(https://www.lampedusa.enea.it/dataaccess/ocean_co2fluxes\), last access: 19 August 2025, 2023.](#)

Perez, F. F., and Fraga, F.: Association constant of fluoride and hydrogen ions in seawater, *Mar. Chem.*, 21, 161–168, [https://doi.org/10.1016/0304-4203\(87\)90036-3](https://doi.org/10.1016/0304-4203(87)90036-3), 1987.

655 [IPCC Special Report on the Ocean and Cryosphere in a Changing Climate, edited by: Pörtner, H.-O., Roberts, D. C., Masson-Delmotte, V., Zhai, P., Tignor, M., Poloczanska, E., Mintenbeck, K., Nicolai, M., Okem, A., Petzold, J., Rama, B., and Weyer, N. M., Cambridge University Press, Cambridge, UK and New York, NY, USA, 755 pp., <https://doi.org/10.1017/9781009157964>, 2019.](#)

Poulson, S. R., and Sullivan, A. B.: Assessment of diel chemical and isotopic techniques to investigate biogeochemical cycles in the upper Klamath River, Oregon, USA, *Chem. Geol.*, 269, 3–11, <https://doi.org/10.1016/j.chemgeo.2009.05.016>, 2010.

660 [Prohić, E., & Juračić, M.: Heavy metals in sediments – problems concerning determination of the anthropogenic influence: study in the Krka River estuary, eastern Adriatic coast, Yugoslavia, *Environ. Geol. Water Sci.*, 13, 145–151, <https://doi.org/10.1007/BF01665136>, 1989.](#)

Ribas-Ribas, M., Battaglia, G., Humphreys, M. P., and Wurl, O.: Impact of nonzero intercept gas transfer velocity parameterizations on global and regional ocean–atmosphere CO₂ fluxes, *Geosciences*, 9, 230, <https://doi.org/10.3390/geosciences9050230>, 2019.

670 Ribas-Ribas, M., Hamizah Mustaffa, N. I., Rahlff, J., Stolle, C., and Wurl, O.: Sea Surface Scanner (S3): A catamaran for high-resolution measurements of biogeochemical properties of the sea surface microlayer, *J. Atmos. Oceanic Technol.*, 34, 1433–1448, <https://doi.org/10.1175/JTECH-D-17-0017.1>, 2017.

Robinson, A. R., and Golnaraghi, M.: The Physical and Dynamical Oceanography of the Mediterranean Sea, in: *Ocean Processes in Climate Dynamics: Global and Mediterranean Examples*, edited by: Malanotte-Rizzoli, P. and Robinson, A. R., Springer Netherlands, 255–306, https://doi.org/10.1007/978-94-011-0870-6_12, 1994.

Con formato: Normal

Con formato: Normal

Con formato: Normal

- 675 Schneider, A., Tanhua, T., Körtzinger, A., and Wallace, D. W. R.: High anthropogenic carbon content in the eastern Mediterranean, *J. Geophys. Res.: Oceans*, 115, C12, <https://doi.org/10.1029/2010JC006171>, 2010.
- Sharp, J. D., Pierrot, D., Humphreys, M. P., Epitalon, J.-M., Orr, J. C., Lewis, E. R., and Wallace, D. W. R.: CO2SYSv3 for MATLAB (v3.1), Zenodo [code], <https://doi.org/10.5281/ZENODO.4023039>, 2020.
- 680 [Shaw, E. C., McNeil, B. I., & Tilbrook, B.: Impacts of ocean acidification in naturally variable coral reef flat ecosystems, *J. Geophys. Res.-Oceans*, 117, C03038, <https://doi.org/10.1029/2011JC007655>, 2012.](#)
- [Soloviev, A., & Lukas, R.: The Near-Surface Layer of the Ocean: Structure, Dynamics and Applications, 2nd Edn., Springer, Dordrecht, the Netherlands, 572 pp., <https://doi.org/10.1007/978-94-007-7620-8>, 2013.](#)
- Stolle, C., Ribas-Ribas, M., Badewien, T. H., Barnes, J., Carpenter, L. J., Chance, R., Damgaard, L. R., Durán
- 685 Quesada, A. M., Engel, A., Frka, S., Galgani, L., Gašparović, B., Gerriets, M., Hamizah Mustaffa, N. I., Herrmann, H., Kallajoki, L., Pereira, R., Radach, F., Revsbech, N. P., ... and Wurl, O.: The MILAN Campaign: Studying Diel Light Effects on the Air–Sea Interface, *Bull. Amer. Meteor. Soc.*, 101, E146–E166, <https://doi.org/10.1175/BAMS-D-17-0329.1>, 2020.
- Takahashi, T., Sutherland, S. C., Chipman, D. W., Goddard, J. G., Ho, C., Newberger, T., Sweeney, C., and
- 690 Munro, D. R.: Climatological distributions of pH, $p\text{CO}_2$, total CO_2 , alkalinity, and CaCO_3 saturation in the global surface ocean, and temporal changes at selected locations, *Mar. Chem.*, 164, 95–125, <https://doi.org/10.1016/j.marchem.2014.06.004>, 2014.
- Takahashi, T., Sutherland, S. C., Sweeney, C., Poisson, A., Metzl, N., Tilbrook, B., Bates, N., Wanninkhof, R., Feely, R. A., Sabine, C., Olafsson, J., and Nojiri, Y.: Global sea–air CO_2 flux based on climatological
- 695 surface ocean $p\text{CO}_2$, and seasonal biological and temperature effects, *Deep Sea Res. Part II: Topical Stud. Oceanogr.*, 49(9–10), 1601–1622, [https://doi.org/10.1016/S0967-0645\(02\)00003-6](https://doi.org/10.1016/S0967-0645(02)00003-6), 2002.
- Van Heuven, S., Pierrot, D., Rae, J. W. B., Lewis, E., and Wallace, D. W. R.: MATLAB Program Developed for CO_2 System Calculations, [software], https://doi.org/10.3334/cdiac/otg.co2sys_matlab_v1.1, 2011.
- Wanninkhof, R.: Relationship between wind speed and gas exchange over the ocean revisited, *Limnol. Oceanogr.: Methods*, 12(6), 351–362, <https://doi.org/10.4319/lom.2014.12.351>, 2014.
- 700 Wong, P. P., Losada, I. J., Gattuso, J.-P., Hinkel, J., Khattabi, A., McInnes, K. L., Saito, Y., & Sallenger, A.: Coastal systems and low-lying areas, in: *Climate Change 2014: Impacts, Adaptation, and Vulnerability. Part A: Global and Sectoral Aspects*, edited by: Field, C. B., Barros, V. R., Dokken, D. J., Mach, K. J., Mastrandrea, M. D., Bilir, T. E., Chatterjee, M., Ebi, K. L., Estrada, Y. O., Genova, R. C., Girma, B.,

Con formato: Normal

705 Kissel, E. S., Levy, A. N., MacCracken, A. N., Mastrandrea, P. R., White, L. L., Cambridge University Press, 361–409, <https://doi.org/10.1017/CBO9781107415379.010>, 2014.

Wurl, O., Landing, W. M., Mustafa, N. I. H., Ribas-Ribas, M., Witte, C. R., & Zappa, C. J.: The Ocean's Skin Layer in the Tropics, in: Journal of Geophysical Research: Oceans, 124(1), 59–74, <https://doi.org/10.1029/2018JC014021>, 2019.

710 Wurl, O., Wurl, E., Miller, L., Johnson, K., & Vagle, S.: Formation and global distribution of sea-surface microlayers, in: Biogeosciences, 8(1), 121–135, <https://doi.org/10.5194/bg-8-121-2011>, 2011.

[Yates, K. K., Dufore, C., Smiley, N., Jackson, C., & Halley, R. B.: Diurnal variation of oxygen and carbonate system parameters in Tampa Bay and Florida Bay, Mar. Chem., 104, 110–124, <https://doi.org/10.1016/j.marchem.2006.12.008>, 2007.](#)

715 Zeebe, R. E., and Wolf-Gladrow, D. A.: CO₂ in Seawater: Equilibrium, Kinetics, Isotopes, Elsevier Oceanography Series, Vol. 65, Elsevier, Amsterdam, ISBN 0444509461, 2001.

[Zutic, V., & Legovic, T.: A film of organic matter at the fresh-water/sea-water interface of an estuary, Nature, 328, 612–614, <https://doi.org/10.1038/328612a0>, 1987.](#)

720

Con formato: Normal